JOURNAL OF MATERIALS SCIENCE 13 (1978) 1887–1900

Low temperature internal friction on γ-irradiated polyvinylidene fluoride (PVDF)

A. CALLENS*
Rijksuniversitair Centrum, B–2020 Antwerpen, Belgium
L. EERSELS, R. DE BATIST†
Materials Science Department, S. C. K./C. E. N., B–2400 Mol, Belgium

A least-squares fitting of the below room temperature part of the internal friction spectra, obtained by the torsion pendulum technique on as-received and γ-irradiated (up to 1 Grad) strips and fibres of polyvinylidene fluoride [$-(CH_2-CF_2-)_n-\ldots$; PVDF] by a superposition of single Debye functions, reveals that the spectral component features are determined not only by purely amorphous chain characteristics but also by the dose-dependence of crystallinity. A careful analysis of the relaxation spectra confirms that at least one relaxation effect (~236 K) is created upon irradiation. The analysis of the dose dependence of the characteristics of the β (glass transition; ~220 K) and β_u (apparent upper glass transition; ~270 K) relaxations, suggests the probable influence of crystallinity on the molecular motion in the amorphous phase. The increase of the intensity of the γ relaxation (~190 K) is related to the irradiation-induced crystallite degradation.

1. Introduction

In a previous paper [1], we have analysed the TSD (thermo-stimulated depolarization) current spectra, recorded on γ-irradiated polyvinylidene fluoride (PVDF) films. Dynamic mechanical experiments, reported below, corroborate the interpretation suggested in [1], but also reveal the possibility that parameters related to crystallinity may influence the relaxation processes, which are attributed to molecular motions of chains within the amorphous phase. This conclusion is arrived at by comparing results belonging to different specimen modifications.

2. Experimental

2.1. Material

While the previous paper [1] described results on 20 μm thin foils, the present one deals with experiments carried out with fibres ($\phi = 280\,\mu m$) and with "bulk" material (1 mm thick plates cut to size suitable for the dynamic mechanical experiments). The crystalline modifications of the bulk and fibre material have been determined by X-ray wide-angle diffraction analysis, according to the literature data of Kosmynin *et al.* [2] and of Tadokoro and co-workers [3, 4]. The α-crystalline modification contains trans-gauche-trans-gauché chain conformations in a monoclinic lattice and may occur in one of two variants, α_o (oriented α) or α_h (high density α). The β crystalline modification is formed mainly in strongly oriented material. The degree of crystallinity χ_{cr} has been determined using Gal'perin's method [5], i.e. comparing the relative fractions of amorphous and crystalline material obtained by estimating their contribution to the area of the X-ray diffraction intensity peaks.

Concerning the fibre materials, no explicit characterization experiments have been carried out but, taking account of their highly oriented structure, it may be presumed that they exhibit an ($\alpha_o + \beta$) modification and a high χ_{cr} value.

*Fellow of the "Interuniversitair Instituut voor Kernwetenschappen"
†Also at Rijksuniversitair Centrum, Antwerpen, Belgium

TABLE I Experimental technique and specimen characteristics

Technique	Material	Crystalline modification	χ_{cr} at zero dose
Kê-pendulum (~ 1 Hz)	fibres ($\phi \sim 280\,\mu m$) length ~ 100 mm	$\alpha_0 + \beta$	highest (strongly oriented)
	bulk strips thickness = 1 mm, length ~ 100 mm, width = 2 mm	α_h	0.58
flexural resonance (10^2 to 10^3 Hz)	bulk strips (length ~ 50 mm)	α_h	0.58
TSD (equivalent frequency ~ 10^{-3} Hz)	films of thickness 20 μm	$\alpha_0 + \beta$	0.44

2.2. Equipment

Dynamic mechanical experiments have been performed by means of both a low-temperature torsion pendulum and flexural resonance equipment.

The Kê-type torsion pendulum [6], enclosed in a vacuum vessel ($p \simeq 1$ Pa) allows measurements in a temperature range between 100 and 300 K. By choosing an appropriate inertia member a frequency of ~1 Hz is obtained for experiments on both fibres and bulk material.

Experiments at higher frequencies have been carried out on bulk strips by semi-automatic recording flexural resonance equipment [7, 8]. The apparatus operates at constant oscillation amplitude, the vibration of the specimen being detected by FM and driven by capacitive coupling (both sides of the specimen, which is mounted as a cantilever, are covered by an evaporated silver layer). The damping is calculated from the required driving force, after comparison with a free-decay run. The experiments are carried out *in vacuo* ($p \simeq 1$ Pa). Table I contains the experimental techniques, the specimen modification and the initial (= zero dose) χ_{cr}-value.

2.3. Irradiation and post-irradiation characterization

The specimens for the dynamic mechanical experiments were γ-irradiated at room temperature by means of spent fuel elements (BR2 reactor, Mol, Belgium; photon energy 1 to 2 MeV; dose rate 7 to 13 Mrad h^{-1}; max. dose ~1 Grad). The post-irradiation characterization has been discussed in

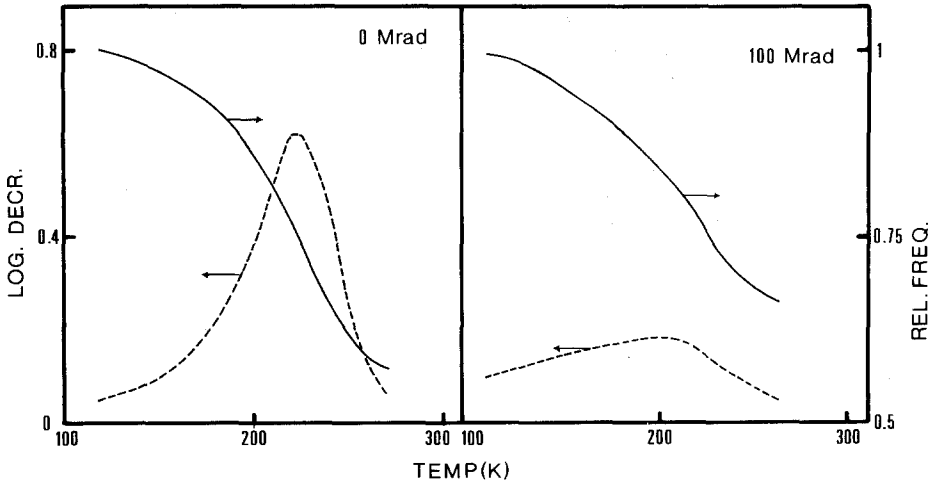

Figure 1 Internal friction and resonance frequency (flexural resonance) for as-received PVDF platelets (a) and 100 Mrad irradiated (b).

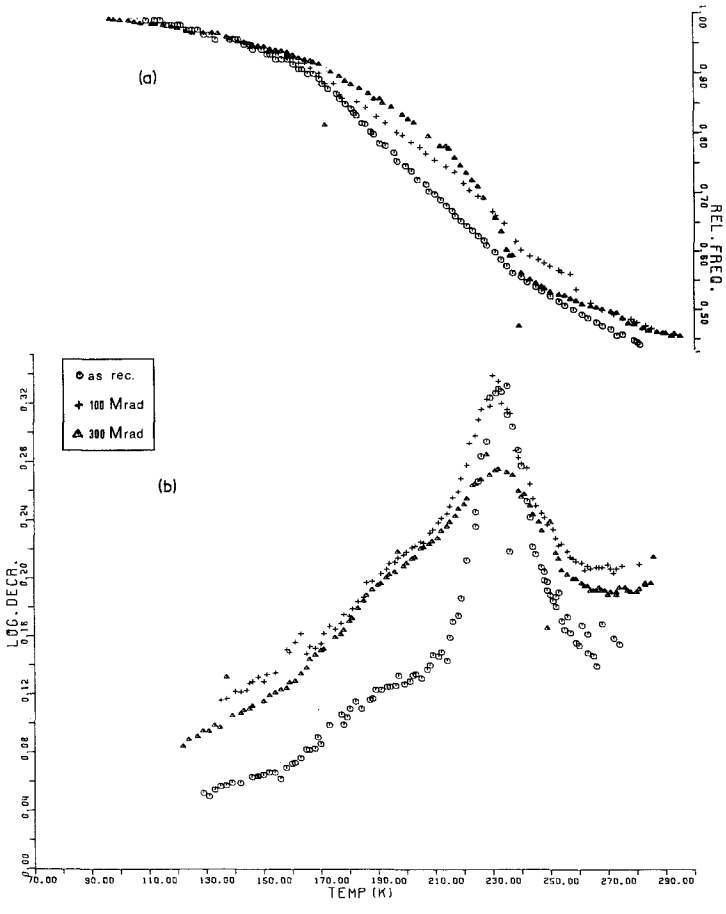

Figure 2 Resonance frequency (a) and internal friction (b) (torsion pendulum) of as-received and γ-irradiated PVDF fibres. The frequency is normalized to unity at 100 K.

[1]; some of the main conclusions are briefly recalled below:

(a) Main chain cross-linking prevails over scission, leading to an increase of the mechanical strength, somewhat depressed by loss of crystallinity at higher doses.

(b) The degree of crystallinity χ_{cr} decreases with increasing dose, resulting in almost complete amorphicisation at 1 Grad.

(c) A strong increase of the infra-red line intensities in the 1500 to 1900 cm^{-1} wavenumber range is attributed to the increase of the contribution of amorphous chains containing multiple bonds, as confirmed by our ESR analysis [9] (creation of fluorinated polyenyl radicals).

3. Experimental results

It is well known (see, for example, [10]) that the resolution of relaxation spectra tends to decrease with increasing measuring frequency so that effects which can be clearly distinguished in TSD spectra (equivalent frequency $\sim 10^{-4}$ to 10^{-3} Hz) are hardly observable in torsion pendulum dynamic mechanical spectra (~ 1 Hz) and even completely merged in flexural resonance spectra ($\sim 10^2$ to 10^3 Hz). Therefore, results obtained by the flexural resonance technique will be considered only if of special importance or complementary to the interpretation of corresponding lower frequency data. Some of the flexural resonance spectra are shown as an example in Fig. 1. The post-irradiation flexural resonance spectra reveal a strong decrease in the relaxation strength, which appears to saturate already at about 100 Mrad. The pre-irradiation peak damping value is very high and results from an extrapolation of the gauge factor obtained for the lower damping temperature regions (the accuracy of a logarithmic decrement derived from a small number of periods is, of course, rather low). Figs. 2a and b represent the damping spectra and the corresponding resonance frequencies (normalized to the value at 100 K) for the fibre material, as obtained by torsion pendulum while Fig. 3a and b show similar results for the bulk platelets. The curves in Figs. 1, 2 and 3 indicate with increasing dose a general

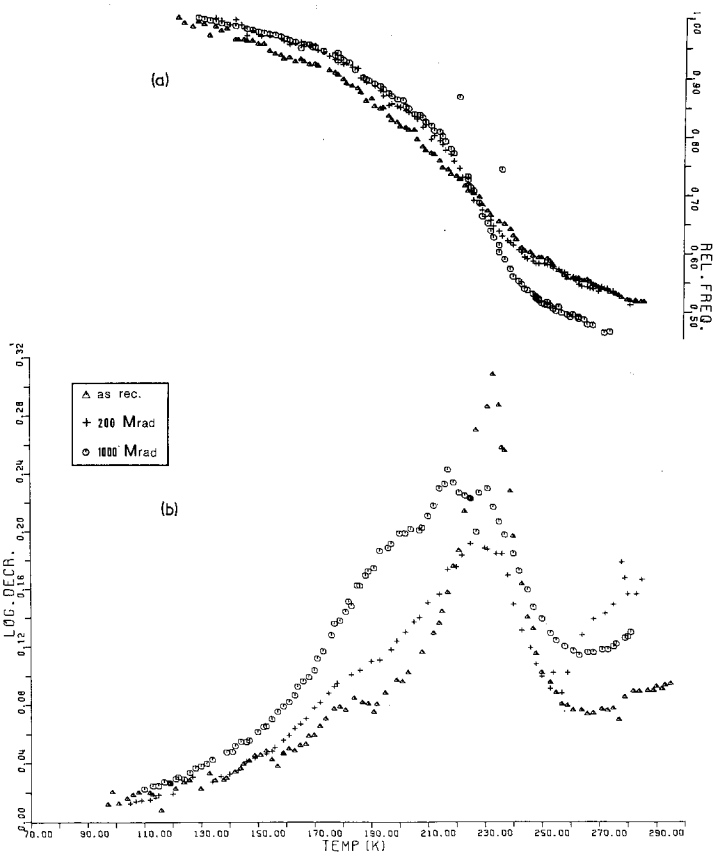

Figure 3 Resonance frequency (a) and internal friction (b) (torsion pendulum) of as-received and γ-irradiated PVDF bulk material. The frequency is normalized to unity at 100 K.

decrease of the intensity, in the whole temperature region considered, as well as an increasing complexity.

4. Analysis of the experimental results

The shape of the torsion pendulum damping spectra clearly suggests the presence of a number of separate contributions. In order to be able to apply a standard computer fitting routine, it has been assumed that the internal friction spectrum may be described by a linear combination of Debye functions:

$$\delta = \sum \delta_{M,i} \frac{x_i}{1 + x_i^2} \qquad (1)$$

in which $\delta_{M,i}$ represents the relaxation strength, ω the pulsation and τ_i $(=x_i/\omega)$ the relaxation time which is an Arrhenius-type function of temperature. The fact that at least one of the components in the temperature range considered may be characterized by a relaxation-time temperature relation which is non-Arrhenius-like (Williams–Landel–Ferry (WLF) behaviour of the β-relaxation [11]) is taken care of by using an effective activation enthalpy (this can be done, since one considers a very restricted ω range).

The distribution of relaxation times, which is usually observed in polymers, has been introduced formally by using a Fuoss–Kirkwood relaxation time distribution function characterized by a parameter m and leading to an apparent activation enthalpy:

$$\Delta H_{a,i} = m\Delta H_i. \qquad (2)$$

This leads to the following expression for the temperature dependence of the damping:

$$\delta(T) = \sum \delta_{M,i} \operatorname{sech} [(\Delta H_{a,i}/k)(T^{-1} - T_{M,i}^{-1})] \qquad (3)$$

in which $T_{M,i}$ are the peak temperatures. As in [1], fitting was done by means of the non-linear least-squares method used in the fitting routine FATAL [12]. To avoid overflow and non-convergence risks during the fit, the natural logarithm of both sides of Equation 3 has been used. As a test for the reliability of the fit, the data have been submitted consecutively to Equation 3 with strongly deviating starting parameters. It is

TABLE II Decomposition of the internal friction spectra, obtained by torsion pendulum on γ-irradiated fibres of PVDF

Dose (Mrad)	Component no.*	$T_{M,i}$(K)	$\Delta H_{a,i}$(eV)	$\delta_{M,i}$ (log. decr.)
0	0	138 ± 3	0.08 ± 0.02	0.052 ± 0.003
	1	194 ± 1	0.13 ± 0.02	0.10 ± 0.01
	3	234 ± 1	0.44 ± 0.01	0.265 ± 0.007
	5	273 ± 0.5	0.59 ± 0.01	0.114 ± 0.004
100	0	127 ± 3	0.043 ± 0.005	0.106 ± 0.003
	1	191 ± 2	0.12 ± 0.01	0.13 ± 0.01
	3	235.5 ± 0.5	0.34 ± 0.02	0.24 ± 0.01
	5	271.5 ± 0.5	0.79 ± 0.04	0.14 ± 0.01
200	0	132 ± 7	0.042 ± 0.005	0.110 ± 0.007
	1	194 ± 3	0.13 ± 0.02	0.14 ± 0.02
	3	233 ± 2	0.35 ± 0.03	0.21 ± 0.02
	5	270 ± 1	0.63 ± 0.06	0.12 ± 0.01
300	0	128 ± 5	0.04 ± 0.01	0.075 ± 0.003
	1	194 ± 4	0.12 ± 0.02	0.10 ± 0.02
	3	233 ± 1	0.30 ± 0.03	0.16 ± 0.01
	5	273 ± 1	0.69 ± 0.08	0.081 ± 0.006
400	0	131 ± 5	0.05 ± 0.01	0.092 ± 0.005
	1	193 ± 4	0.13 ± 0.02	0.14 ± 0.02
	3	235 ± 1	0.28 ± 0.04	0.18 ± 0.02
	5	272 ± 1	0.78 ± 0.06	0.09 ± 0.01

*To maintain the similarity with the bulk results we have used the same labelling, so that Component no. 4 has been omitted in this list, since it has not been observed as a separate contribution.

TABLE III Decomposition of the internal friction spectra, obtained by torsion pendulum on γ-irradiated bulk strips of PVDF

Dose (Mrad)	Component no.	$T_{M,i}$(K)	$\Delta H_{a,i}$(eV)	$\delta_{M,i}$(log. decr.)
0	0	134 ± 7	0.04 ± 0.01	0.025 ± 0.005
	1	195 ± 5	0.12 ± 0.04	0.07 ± 0.01
	3	231 ± 1	0.50 ± 0.03	0.24 ± 0.01
	5	278 ± 1	0.73 ± 0.07	0.050 ± 0.005
200	0	158 ± 10	0.03 ± 0.01	0.024 ± 0.004
	1	189 ± 2	0.13 ± 0.02	0.075 ± 0.008
	3	224 ± 2	0.31 ± 0.03	0.12 ± 0.02
	4	236 ± 2	0.9 ± 0.3	0.04 ± 0.03
	5	275 ± 1	0.72 ± 0.08	0.12 ± 0.01
400	0	140 ± 10	0.05 ± 0.01	0.030 ± 0.005
	1	188 ± 4	0.13 ± 0.02	0.09 ± 0.02
	3	220 ± 7	0.30 ± 0.10	0.08 ± 0.03
	4	237 ± 2	0.5 ± 0.2	0.07 ± 0.04
	5	270 ± 1	0.76 ± 0.08	0.097 ± 0.004
700	0	137 ± 10	0.04 ± 0.01	0.032 ± 0.009
	1	186 ± 10	0.13 ± 0.03	0.108 ± 0.05
	3	216 ± 7	0.27 ± 0.05	0.085 ± 0.01
	4	238 ± 5	0.4 ± 0.1	0.096 ± 0.03
	5	275 ± 1	0.8 ± 0.1	0.071 ± 0.006
1000	0	144 ± 10	0.050 ± 0.005	0.037 ± 0.005
	1	194 ± 5	0.14 ± 0.02	0.14 ± 0.025
	3	218 ± 3	0.4 ± 0.1	0.08 ± 0.03
	4	236 ± 3	0.4 ± 0.1	0.09 ± 0.02
	5	271 ± 1	0.6 ± 0.1	0.060 ± 0.006

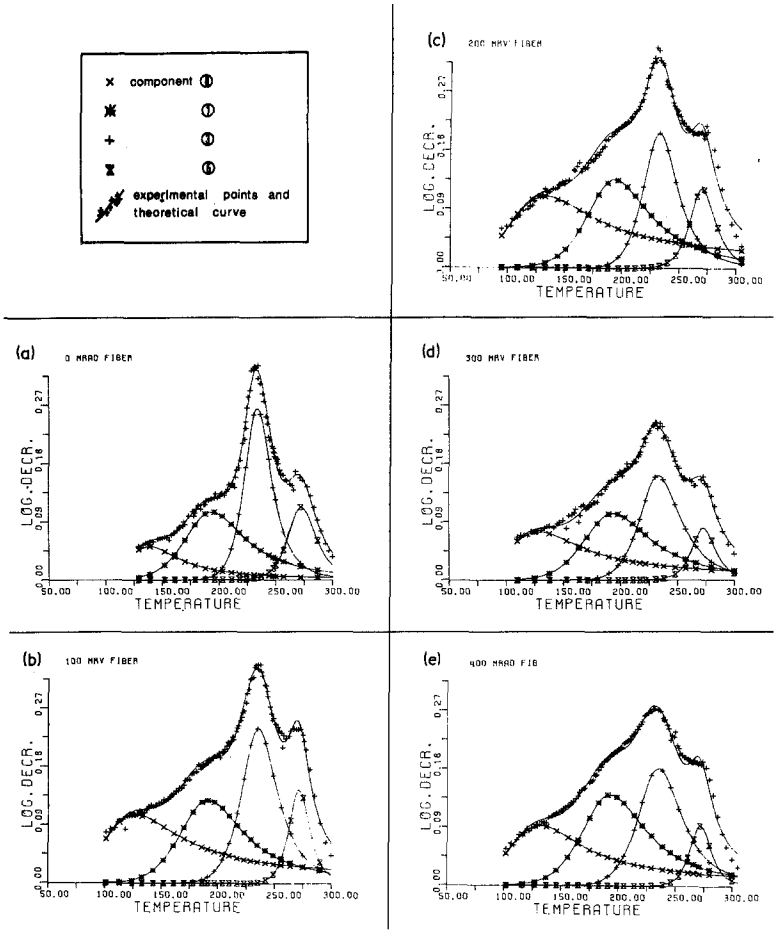

Figure 4 Decomposition of the internal friction spectra of as-received and γ-irradiated PVDF fibres into their components. (a) 0 Mrad; (b) 100 Mrad; (c) Mrad; (d) 300 Mrad; (e) 400 Mrad.

satisfying that a strong coherence in the final parameter values is obtained (see Tables II and III, corresponding to fibre and bulk results, respectively). Figs. 4 and 5 contain some selected post-irradiation spectra, the separate individual components and their sum, calculated by Equation 3. Fig. 5 and Table III, indicate the presence of at least one irradiation-created component in the bulk material spectra. The interpretation for the dose-dependent behaviour of the various components is given separately. Most attention has been paid to the dose dependence of the relaxation strengths, presented in Fig. 6. Occasionally, the dose dependence of other parameters ($T_{M,i}$, $\Delta H_{a,i}$) will be incorporated when it contains supplementary information useful for the interpretation.

5. Discussion of the experimental results

The data of Tables II and III and Fig. 6 may be interpreted along the lines developed for the analysis of the post-irradiation TSD data [1]. In the subsequent analysis, the components have been labelled 0 to 5, in correspondence with the sequence adopted in [1].

5.1. Component no. 0 (not present in [1])

This component should not be considered as a "true" relaxation effect, but rather as a correction term, which takes account of the background damping. Its intensity (Fig. 6a) is about three times as large for the fibres as for the bulk material, which may be explained by the much smaller mass of the former type of specimen.

5.2. Component no. 1

Its position ($T_{M,1} \sim 190$ K) and the value of its apparent activation enthalpy ($\Delta H_{a,1} \sim 0.13$ eV), which remain practically unaltered by irradiation, suggest that this component corresponds to the γ-relaxation. From Fig. 6b, it appears that the relaxation strength gradually increases with dose. This may be understood in terms of the cranck-shaft or local-mode molecular models [1, 11] based

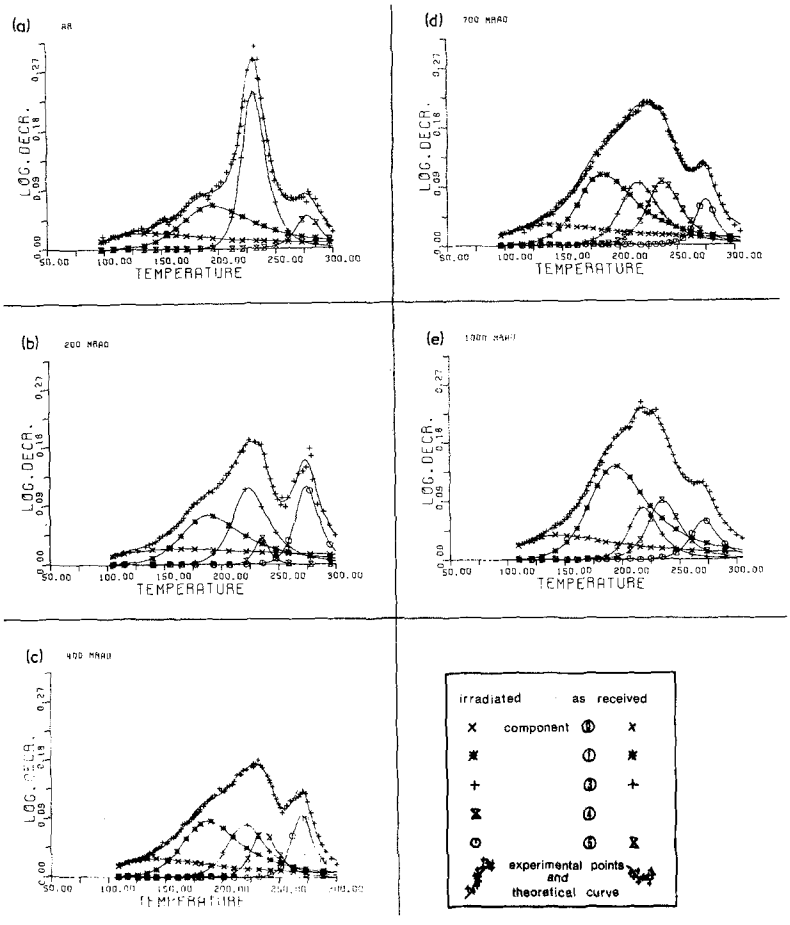

Figure 5 Decomposition of the torsion pendulum internal friction spectra of as-received and γ-irradiated PVDF bulk platelets into their components. (a) 0 Mrad; (b) 200 Mrad; (c) 400 Mrad; (d) 700 Mrad; (e) 1000 Mrad.

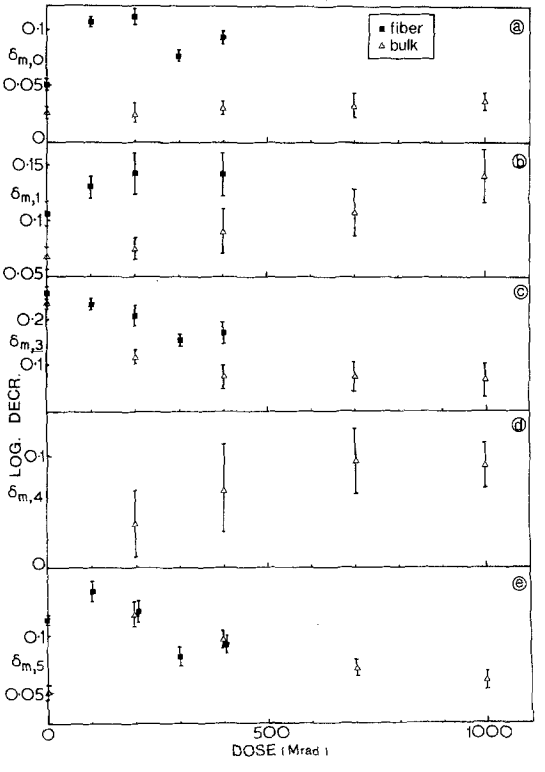

Figure 6 The dose dependence of the intensities of the components of the as-received and post-irradiation internal friction spectra.

upon molecular motions of small (2 to 4 monomer units), isolated chain segments within the amorphous fraction of the material. The loss of crystallinity may then explain the increase with dose of $\delta_{M,1}$ [13].

5.3. Component no. 3

As observed from Figs. 4, 5 and 6 and Tables II and III, the general decrease of the intensity of the below room temperature relaxation region with dose is almost exclusively due to this component, which corresponds to the β-relaxation (glass-transition T_g) [11]. From the dose dependence of its parameters, listed in Tables II and III, several characteristic features may be deduced:

(a) a broadening of this relaxation peak (Section 5.3.1.);

(b) a strong decrease of the peak intensity (Section 5.3.2.);

(c) a downward shift of the peak temperature (Section 5.3.3.).

The interpretation of all of those features can be related to changes in the chain length distribution, introduced schematically in [1].

5.3.1. The broadening of the internal friction β-peaks

This broadening with dose (see also [14]) may be expressed by means of the dose dependence of the distribution parameter:

$$m_\beta = \Delta H_{a,3}/\Delta H_{eff,3}. \quad (4)$$

$\Delta H_{a,3}$ is the dose-dependent apparent activation enthalpy derived from the computer fit and $\Delta H_{eff,3}$ ($\sim$1.85 eV) has been estimated from the apparent linearity of the WLF curve in the limited frequency range of the torsion pendulum experiments for an as-received material [15]. From Fig. 7, it appears that the decrease of m_β saturates above a dose of 200 Mrad. (The 1 Grad data point is difficult to assess since the material has almost completely degraded at this dose.) We suggest that this irradiation-enhanced peak broadening may be attributed to the absorption into the post-irradiation β-peak of at least one of the two irradiation-created TSD effects (see Components no. 2 and no. 4; Section 7 in [1]). An apparently similar phenomenon with a different interpretation has been reported by Ishida *et al.* [16], who observed a broadening of the dielectric relaxation peaks for a series of cross-linked or blended semi-crystalline polymers. They attributed this broadening to an alteration of the molecular chain force constants and friction coefficients.

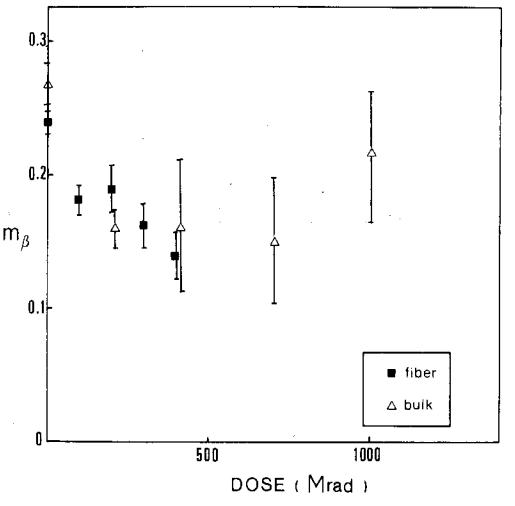

Figure 7 Dose dependence of the Fuoss–Kirkwood broadening parameter m_β of the β-peak.

5.3.2. The decrease of intensity of component no. 3

The decrease of the intensity of Component no. 3 (Fig. 6c) is different in aspect for the various material modifications, as seen from Fig. 8, which presents several post-irradiation β-intensities, all normalized to their zero dose value. To account for this decrease, we have proceeded in two ways.

5.3.2.1. In the first approach [14], use is made only of the dose dependence of the relaxation strength. It assumes a proportionality between the relaxation strength $\delta_{M,3}$ and the free molecular length L_c between cross-links. In the case of a polymer which predominantly cross-links upon irradiation, L_c is approximately inversely proportional to the cross-linking density $x(R)$ [17]. Rather than using the generally accepted [18] linear dose dependence of $x(R)$, we have extended it to larger dose values and have incorporated both saturation effects and pre-irradiation cross-links:

$$x(R) = u\{c_0 + c_1[1 - \exp(-R/R_0)]\}. \quad (5)$$

The parameters in this intuitively derived expression can be interpreted in terms of physical quantities; u is the zero dose molecular length ($= \bar{M}_n/M$, $\bar{M}_n$ being the number average poly-

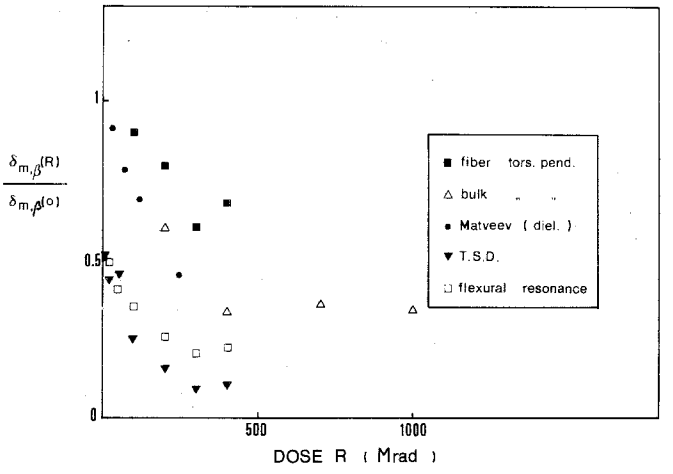

Figure 8 Post-irradiation intensities of the β-peak, obtained by TSD, dielectric relaxation technique and dynamic mechanical techniques, normalized to unity at zero dose.

TABLE IV Determination of post-irradiation cross-linking parameters from the dose dependence of the β-peak intensities (first approach of analysis)

Parameter	c_0	c_1	R_0 (Mrad)	c_0/c_1
T.S.D.	2×10^{-3}	1.3×10^{-2}	113	0.16
Flexural resonance* (bulk)	2×10^{-3}	6.5×10^{-3}	65	0.31
Dynamic mechanical (bulk tors. pend.)	3.3×10^{-3}	4.6×10^{-3}	83	0.72
Dynamic mechanical (fibres tors. pend.)	5×10^{-3}	3.7×10^{-3}	300	1.06

*Those results are based on the average total relaxation strength which cannot be completely resolved

TABLE V Post-irradiation $\alpha(R)$-values of PVDF

Material modification	Dose (Mrad)														
	0	5	10	20	30	50	60	100	120	200	240	300	400	700	1000
TSD (20 μm films) α_{TSD}	0.85	0.66	0.41	0.35		0.29		0.20		0.14		0.11	0.08		
Matveev (dielectric relax. bulk) α_{diel}	0.94				0.85		0.70		0.57		0.40				
this work (torsion pendulum–bulk) α_{mech}	0.94									0.40			0.31	0.38	0.27
this work (torsion pendulum–fibres) α_{mech}	0.9							0.88		0.73		0.63	0.72		

mer and M the monomer molecular weights), c_0 is related to the initially present cross-linking (or other chain motion hindering effects), c_1 to the radiation-induced chain motion hindering and R_0 charasteristic for the rate of saturation. From Equation 5:

$$L_c \propto ux^{-1} = \{c_0 + c_1 [1 - \exp(-R/R_0)]\}^{-1} \quad (6)$$

and hence:

$$\delta_{M,3} = K_c\{c_0 + c_1 [1 - \exp(-R/R_0)]\}^{-1}. \quad (7)$$

Equation 7 is, of course, only a very crude description of the experimental reality, yet it yields

estimates for parameter values to be introduced in a more sophisticated model. Table IV contains the c_0, c_1, R_0 parameter values obtained from a fit of the experimental intensities listed in Tables II and III, complete with TSD results of [1] and also with flexural resonance data. A discussion of the final parameter values will be done after the analysis with the more elaborate method.

5.3.2.2. The second way of analysing the dose dependence of the β-intensities is based on the development of expressions for the post-irradiation molecular size distributions. It is an extension of the preliminary considerations developed in [1] (Section 7, Component no. 3). It will be more extensively discussed in a separate paper and essentially consists in determining the fraction of amorphous material $\alpha(R)$ taking part in the chain segmental micro-Brownian motions (β-relaxation). $\alpha(R)$ is calculated from the post-irradiation molecular size distributions $Z(p, x, y)$, where p is the molecular length, x the cross-linking density and y the scission density. $\alpha(R)$ may be evaluated analytically in some specific cases, of which the one corresponding to a zero-dose molecular size distribution of the "random" type $[\alpha_2(R)]$ is the most suitable. This is not surprising since $\alpha_2(R)$ is derived from the most simple zero dose distribution function $Z(p, 0, 0)$ and contains both the cross-linking and scission densities:

$$\alpha_2(R) = \exp(-V)\left\{1 + \frac{xV(V^2 + 3V + 6)}{6[(1 + 2\Delta x)B^3 + x]}\right\} \quad (8)$$

wherein:

$$B = [1 + (\Delta + 2)x]; \; V = (p_c/u)B; \; \Delta = y/x$$

with Δ the ratio of scission to cross-link densities and p_c a critical molecular length, i.e. the minimum length of the amorphous chain segments to be allowed to take part in the collaborative reorganization at T_g. Introducing Equation 7 into Equation 8 yields the dose dependence for the $\alpha(R)$ expressions. The theoretical expressions of $\alpha(R)$ are determined by five parameters, i.e. p_c, Δ, c_0, c_1, R_0. The experimental $\alpha(R)$-values may be determined from:

$$\alpha(R) = N_D/N_T \quad (9)$$

where N_D is the number of monomer units taking part in the relaxation and N_T the total number of monomer units. In [1], we have derived an $\alpha(R)$ for the TSD results:

$$\alpha_{TSD}(R) = K_{TSD}\frac{Q_\beta T_{M,3}}{(1 - \chi_{cr})} \quad (10)$$

with K_{TSD} a factor which is to a first approximation independent of dose and determined by poling factors and geometrical constants; Q_β is the charge release over the β peak. The experimental $\alpha(R)$ values for TSD are listed in Table V. We have also attempted to evaluate $\alpha(R)$ from the dielectric relaxation results of Matveev *et al.* [19] obtained on bulk PVDF. The $\alpha(R)$ values have been calculated from Equation 9, taking account of the Onsager–Kirkwood Equation for the dielectric relaxation strength [20]:

$$\alpha_{diel}(R) = K_{diel}\frac{T_{M,3}(2\epsilon_s + \epsilon_\infty)(\epsilon_s - \epsilon_\infty)}{g(1 - \chi_{cr})\epsilon_s(\epsilon_\infty + 2)^2} \quad (11)$$

K_{diel} contains the factors which are independent of dose in a first approximation; ϵ_s and ϵ_∞ are the relative dielectric constants at very low and very high frequency; g the Fröhlich interaction parameter which takes account of orientational effects due to nearest-neighbour molecules.

The dose dependent $\alpha_{diel}(R)$ values, calculated from the experimental data of Matveev *et al.* [19], are also listed in Table V.

The internal friction data are difficult to evaluate on the basis of Equation 9, since the necessary numerical values of quantities, such as the mechanical dipolar moment, are not known. Nevertheless $\alpha_{mech}(R)$ may be calculated from the mechanical relaxation peaks on the basis of a model developed by Gisolf *et al.* [21–23]. They assume a proportionality between the concentration of mobile monomer units and the area under the loss compliance peak:

$$\alpha_{mech}(R) \propto \int_{\text{loss peak}} D''(\ln \omega)\mathrm{d}(\ln \omega) \quad (12)$$

with D'' the loss compliance and ω the angular frequency. It may be demonstrated that Equation 12 may be rewritten in terms of temperature T as the independent variable. When using discrete variables and considering an Arrhenius-like single relaxation time effect, Equation 12 becomes:

$$\alpha_{mech}(R) \propto \sum_{i=1}^{N} \delta(T_i)f^2(T_i)T_i^{-2}(\Delta T)_i \quad (13)$$

with N the number of experimental data points

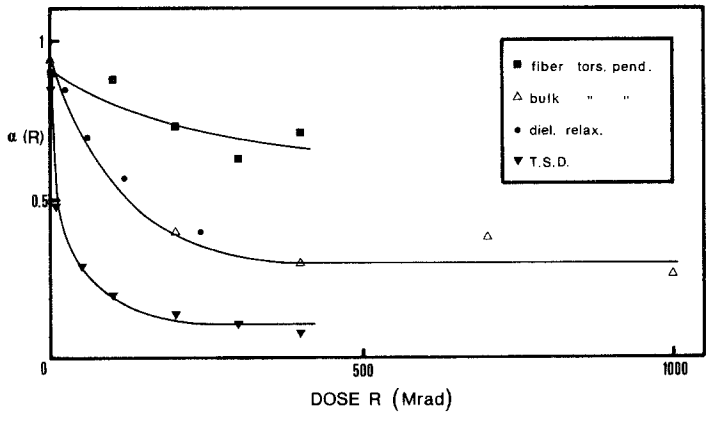

Figure 9 Dose dependence of the post-irradiation $\alpha(R)$ values, superimposed with the theoretical curves.

covering the β internal friction peak. $T_i, \delta(T_i), f(T_i)$ and $(\Delta T)_i$ are, respectively, the temperature, damping value, frequency and temperature step at each experimental point. This method does not allow an absolute determination of the $\alpha_{mech}(R)$ values for each dose, but only relative to a reference, say α_{mech} (0). The value of α_{mech} (0) of the bulk platelets has been assumed to be equal to the one obtained for the dielectric relaxation data of Matveev *et al.*, listed in Table V [α_{diel} (0) ~0.94]. The zero dose α_{mech} (0) value for the fibres was not available and has been estimated very roughly to be 0.9. Both series of α_{mech} (R) values, obtained for the torsion pendulum results, are also listed in Table V.

The experimental $\alpha(R)$ values, listed in Table V, and shown versus dose in Fig. 9, have been submitted to a mathematical fit with Equation 8. The high-dose values α_{mech} (R) for the fibres have probably been overestimated, if one considers the possible influence of neighbour effects on the β-peak as pointed out in Section 5.3.1. This may explain the exaggerated difference between the two curves, corresponding to the dynamic mechanical results. Only in the case of the TSD experiments, a sufficient number of data were available to carry out the fit with all five parameters $[p_c, \Delta, c_0, c_1, R_0]$ while for both series of torsion pendulum data, one of them has been fixed to reduce non-convergence risks. To try out the reliability of the latter fits, different parameters were fixed consecutively during the computer runs of the fit, leading to acceptable final parameter values, which are all listed in Table VI. From this table, there appears to be surprisingly good agreement between the results, taking account of the limited number of data points and the often limited reliability of the experimental $\alpha(R)$ values.

TABLE VI Parameter values obtained from the curve fitting of the post-irradiation $\alpha(R)$ values of PVDF

Experimental results	Parameter					
	p_c	Δ	c_0	c_1	R_0 (Mrad)	c_0/c_1
TSD (α_{TSD})	43	0.35	3×10^{-3}	1.8×10^{-2}	70	0.17
dielectric relax. α_{diel}	(fixed) 43	0.31	5×10^{-3}	8×10^{-3}	130	0.62
(Matveev *et al.*)	34	(fixed) 0.35	5×10^{-3}	1.5×10^{-2}	200	0.33
dynamic mech. α_{mech}	(fixed) 43	0.31	2.8×10^{-3}	1.1×10^{-2}	126	0.25
(bulk strip)	37	(fixed) 0.35	2.8×10^{-3}	1.3×10^{-2}	126	0.21
dynamic mech. α_{mech}	(fixed) 43	0.31	5×10^{-3}	3.4×10^{-3}	165	1.47
(fibres)	43	(fixed) 0.35	4.8×10^{-3}	3×10^{-3}	160	1.60

The value of p_c in Table VI (34 to 43 monomer units) is somewhat higher than theoretical estimates of Brydson [24] and Boyer [25] [~20 to 30 μm]. The value of $10^3 c_0$ remains between 3 and 5 independent of specimen modification or applied technique, which suggests that c_0 may be a material constant. c_1 and R_0 clearly are related to differences in initial steepness and rate of saturation of the curves of Fig. 8. This may also be expressed by evaluating c_0/c_1 (Table IV), which points to a correlation with the degree of crystallinity χ_{cr} (Table I). This suggests that the radiation damage is the least effective for a high initial crystallinity. It is clear that the correlation presented here is very rough, since it may be assumed that not only χ_{cr} plays a role but also the shape and size of the crystallites and their dispersion within the amorphous phase. In [26], it is shown that there is a fairly good correlation between physical quantities calculated from the parameter values of Table VI and equivalent data determined from post-irradiation solution experiments.

Tables IV and VI show that the c_0/c_1 values obtained with both analysis techniques exhibit the same trends, although in specific cases (e.g. torsion pendulum–bulk) they may strongly differ among each other.

5.3.3. The dose dependence of the peak temperatures $T_{M,3}$

This dependence for both series of dynamic mechanical experiments is represented in Fig. 10. While for the fibres, $T_{M,3}$ remains about constant, one observes a dose-dependent decrease for the bulk material, the latter results somewhat confirming the trend observed for the TSD results [1]. To account for this downward temperature shift, we have proceeded on the basis of a formalism developed by Boyer [25] relating the shift of the glass transition temperature (T_g, here $T_{M,3}$) to what is vaguely defined as the "mid-chain" molecular length n:

$$T_{M,3}/T_g(\infty) = (n+2)/(n+2K_g^{-1}). \quad (14)$$

$T_g(\infty)$ is the transition temperature for an infinite molecular length; K_g has been defined as a dimensionless parameter with a value between (0.5 to 2) and (4 to 8) for semi-crystalline polymers containing, respectively, mainly completely free amorphous chains and mainly chains closed on the crystallite surface. For $n \gg 2$ and after replacement of n by the free length L_c between cross-links, Equation 14 becomes:

$$T_{M,3} \simeq T_g(\infty)[1 + 2L_c^{-1}(1 - K_g^{-1})]. \quad (15)$$

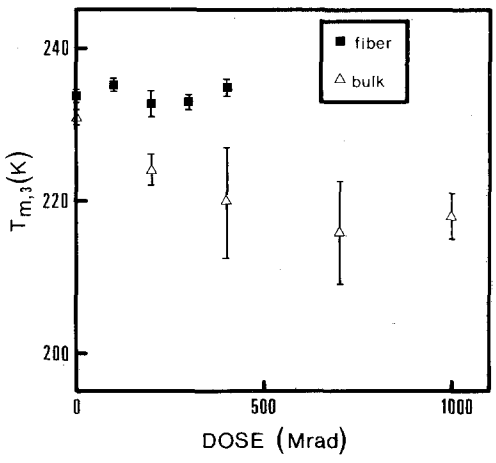

Figure 10 Dose dependence of β peak temperature $T_{M,3}$ obtained by the various relaxation techniques.

Fitting the experimental data of Fig. 10 and those given in [1] with L_c values determined from Equation 6, with the introduction of parameter values listed in Table VI, yields final values for K_g and $T_g(\infty)$ listed in Table VII. The values of $T_g(\infty)$ are in the expected range, while the K_g values do not confirm completely the expected correlation with degree of crystallinity χ_{cr}. They do, however, suggest that initially only free amorphous chains take part in the relaxation effect.

TABLE VII

	Films (TSD)	Fibres (torsion pendulum)	Bulk strip (torsion pendulum)
$T_g(\infty)$	225 K	236 K	240 K
K_g	0.4	0.64	0.17

5.4. Component no. 4

This component can be observed as a separate peak only in the "bulk" results presented in Fig. 3a. The dynamic mechanical Component no. 4 has nearly similar characteristics to its equivalent in the post-irradiation TSD spectra, i.e. it is apparently sharper than the neighbouring peaks (higher apparent activation enthalpy) and it presents only a very small shift of the peak temperature. If one calculates the activation enthalpy from the frequency versus $T_{M,4}^{-1}$ relationships of the TSD results (232 K; 10^{-3} Hz) and the bulk torsion pendulum data (237 K; 0.7 Hz), one obtains an unreasonably high value of 15 eV.

One may interpret those features on the basis of either one of two hypotheses. The first one assumes that the high apparent activation enthalpy corresponds to the low temperature tail of some kind of WLF-curve for the chain segments containing multiple bonds, which may execute a cooperative Brownian motion, corresponding to a kind of glass transition; this has already been suggested in [1]. The second hypothesis is that the observed high activation enthalpy is due to the fact that the peak corresponds to a second-order thermodynamic transition, for which, however, no acceptable mechanism seems conceivable. The results of the characterization, given in Section 2.3, are in favour of the first hypothesis, since they reveal a gradual increase of the amount of unsaturation upon increasing dose. As already pointed out during the analysis of Component no. 3, it is plausible that fibre Component no. 3 has absorbed TSD Components no. 2 and no. 4 [1] and that bulk Component no. 3 has absorbed TSD Component no. 2, as observed from the apparent broadening of the β-peak, mentioned above.

5.5. Component no. 5

The highest temperature component of the low temperature internal friction spectrum is difficult to assess because of cut-off difficulties from the above room temperature part of the spectrum, which exhibits much higher levels of damping for doses exceeding 400 Mrad. Then, it is surprising that there is still such a good agreement in the shapes of the intensity curves of Fig. 6e which both exhibit a maximum at $\simeq 100$ Mrad. The corresponding TSD results of [1] only show an initial flattening with dose and a subsequent decrease, comparable to the torsion pendulum results.

In [1], we have attributed Component no. 5 to the (apparent) upper glass transition β_u [$T_g(u)$ in [1]]. The phenomenological interpretation of the above features is in accordance with this β_u hypothesis. The initial intensity increase in Fig. 6e may indeed be attributed to the incorporation into the β_u effect of amorphous chains, produced by the initial cross-linking, which do not exceed the critical chain length p_c, to take part in the β-relaxation (Component no. 3), but which are long enough to belong to β_u, which, according to Boyer [25], is performed by shorter amorphous chain segments. The subsequent decrease of the intensity may be explained within the same framework developed for the β-relaxation, i.e. a hindering of the molecular chain Brownian motion through the creation of the cross-linking network. That the decrease of the intensity is much less steep than for the β_u-relaxation may be explained through one of the characteristic features of β_u, i.e. the hindering of the molecular motion by the crystallites [26], which depresses the importance of subsequent hindering brought about by the radiation cross-linking. The above hypothesis needs further quantitative confirmation.

Acknowledgements

The authors wish to thank the Research Division of Solvay, especially Dr Majot for their kindness in supplying the specimens. They thank Mr Gandolfo and Mr Boeykens (BR2-Mol) for the irradiations and Drs P. Nagels and J. Nihoul for a critical reading of the manuscript. One of them (A.C.) is grateful to I.I.K.W. for having obtained a fellowship.

References

1. A. CALLENS, R. DE BATIST and L. EERSELS, *J. Mater. Sci.* **12** (1977) 1361.
2. B. P. KOSMYNIN and Y. L. GAL'PERIN, *Vysokomol. Soyed.* **A14** (1972) 1603.
3. R. HASEGAWA, Y. TAKAHASHI, Y. CHATANI and H. TADOKORO, *Polymer J.* **3** (1972) 600.
4. M. KOBAYASHI, K. TASHIRO and H. TADOKORO, *Macromolecules* **8** (1975) 158.
5. Y. L. GAL'PERIN, B. P. KOSMYNIN and V. K. SMIRNOV, *Vysokomol. Soyed* **A12** (1970) 1880.
6. R. DE BATIST "Internal friction of structural defects in crystalline solids" (North-Holland, Amsterdam, 1972) p. 83.
7. L. CLAESSEN and J. WIJSMANS, "Regeneratief systeem voor het kontinu meten van de inwendige wrijving, gebruik makend van een F.M. techniek" Techn. Eng. Thesis (T.I.H.H., Hasselt, Belgium, 1971).
8. L. EERSELS and R. DE BATIST, unpublished.
9. A. CALLENS, unpublished data.
10. J. VAN TURNHOUT, "Thermally stimulated depolarization of polymer electrets" (Elsevier, Amsterdam, 1975) p. 59.
11. A. CALLENS, R. DE BATIST and L. EERSELS, *Il Nuovo Cimento* **33B** (1976) 434.
12. L. SALMON and D. V. BOOKER "Subroutine FATAL" AERE-R 7219 (1972).
13. G. W. DEELEY, J. A. SAUER and A. E. WOODWARD, *J. Appl. Phys.* **29** (1958) 1415.
14. A. CALLENS, R. DE BATIST and L. EERSELS, paper presented at the 6th ICIFUAS Meeting (Tokyo, July, 1977).

15. A. CALLENS, unpublished results.
16. Y. ISHIDA, K. SHIMADA, M. TAKAYANAGI and K. YAMAFUJI, Repts. Progr. in Polym. Phys. in Japan **VI** (1963) 237.
17. T. YOSHIDA, R. E. FLORIN and L. A. WALL, *J. Polymer Sci.* **A3** (1965) 1685.
18. A. CHARLESBY and S. H. PINNER, *Proc. Roy. Soc.* **A249** (1959) 367.
19. V. R. MATVEEV, S. E. VAISBERG and V. L. KARPOV, *Soviet Plastics* **9** (1971) 48.
20. VON HIPPEL, "Dielectrics and Waves" (J. Wiley, New York, 1954) 181.
21. J. H. GISOLF, *Colloid Polymer Sci.* **253** (1975) 185.
22. *Idem,* Delft Progr., Rep. Series **A1** (1976) 125.
23. J. L. KALWAK, D. J. VAN DIJCK and J. H. GISOLF, *ibid.* **A1** (1976) 131.
24. J. A. BRYDSON, "Polymer Science" (ed. A.D. Jenkins) (North-Holland, Amsterdam, 1972) ch. 3.
25. R. F. BOYER, *J. Polymer Sci. symp.* **50** (1975) 189.
26. A. CALLENS and R. DE BATIST, results to be submitted for publication.

Received 9 November and accepted 16 December 1977.